THERMAL PERFORMANCE OF PANELS WITH HIGH DENSITY, RANDOMLY ORIENTED STRAW BALES

Sarah Seitz,[1] Kyle Beaudry[2], and Colin MacDougall,[3]

ABSTRACT

This paper describes the hot-box testing (based on ASTM C1363-11) of seven straw bale wall panels to obtain their thermal conductivity values. All panels were constructed with stacked bales and cement-lime plaster skins on each side of the bales. Four panels were made with traditional, 2-string field bales of densities ranging from 89.5 kg/m^3–131 kg/m^3 and with the bales on-edge (fibres perpendicular to the heat flow). Three panels were made with manufactured high-density bales (291 kg/m^3–372 kg/m^3). The fibres of the manufactured bales were randomly oriented.

The key conclusion of this paper is that within the experimental error, there is no difference in the thermal conductivity value for panels using normal density bales and manufactured high density bales up to a density of 333 kg/m^3. However, because of lack of precision of the hot-box, no conclusions can be made on the true thermal conductivity of the high density bale panels. In addition, the panels tested were found to have significant voids between bales, and this is believed to have contributed to higher measured thermal conductivity values compared to those reported in the literature for normal density bale panels. Thermal properties may be affected for bales with higher densities than 333 kg/m^3, therefore further testing is suggested.

KEYWORDS

straw bale construction, thermal testing, thermal conductivity, hot-box apparatus, high-density bales

INTRODUCTION

The building industry is responsible for approximately 40% and 33% of the global energy consumption and greenhouse gas (GHG) emissions, respectively (UNEP, 2009). Conversely, it is also the sector with the largest potential to reduce these parameters using currently available technologies. (UNEP, 2009)

Sartori & Hestnes (2007) and Ramesh et al. (2010) have compared Life Cycle Assessments (LCA) of residential buildings and have found that their energy consumption is dominated by the operational phase, which includes all the energy consumed after the construction until the

1. Sarah Seitz, PhD Candidate, Dept. of Civil Engineering, Queen's University, Kingston, Ontario, Canada
2. Kyle Beaudry, M.A.Sc. Candidate, Dept. of Civil Engineering, Queen's University, Kingston, Ontario, Canada
3. Colin MacDougall, Associate Professor, Dept. of Civil Engineering, Queen's University, Kingston, Ontario, Canada (corresponding author, macdougc@queensu.ca).

demolition or recycling. Furthermore, the United Nation Energy Programme suggests that 60% of the energy of the operational phase is used for space heating (UNEP, 2009).

With the recent push for sustainable engineering from programs such as Leadership in Energy and Environmental Design (LEED), more studies are being performed on the benefits of energy efficient homes. Offin (2010) compared the embodied energy of a post-and-beam straw bale wall (SBW) and a typical timber frame (TTF) with vinyl finish and determined that the SBW embodied 676 MJ less than the TTF, which was nearly 60% of the TTF embodied energy. Blanchard & Reppe (1998) performed a LCA comparing a standard home (SH) and energy efficient home (EEH) located in Ann Arbor, Michigan, and concluded that the life cycle energy and life cycle global warming potential of a EEH is reduced by a factor of 2.73 and 2.71, respectively. The authors also state that the most efficient strategy to reduce a home's heating energy consumption is by implementing better insulation. One possible sustainable solution for greater thermal performance would be using straw bale walls. Magwood (2014) suggests that straw bale walls are energy efficient due to their high thermal resistance (R-value), in addition to having reduced embodied energy, and contributing to indoor air quality.

The application of straw bale construction has become popular worldwide with over 1,670 registered buildings in 2017 (Sustainable Sources, 2017). Briefly, straw bale walls consist of stacked bales with thin plaster membranes (which may be earthen or lime-cement, and which may be reinforced or unreinforced) on each side (Figure 1). The bales may be stacked "flat" or "on-edge" (Figure 2). However, there is no "standard" method for constructing straw bale walls, and there is a wide range in the characteristics (size, density, moisture content, etc.) of straw

FIGURE 1. Typical straw bale wall (ICFHome, 2017).

FIGURE 2. Fiber orientation of regular 2-string bale on-edge (left) and laid flat (right).

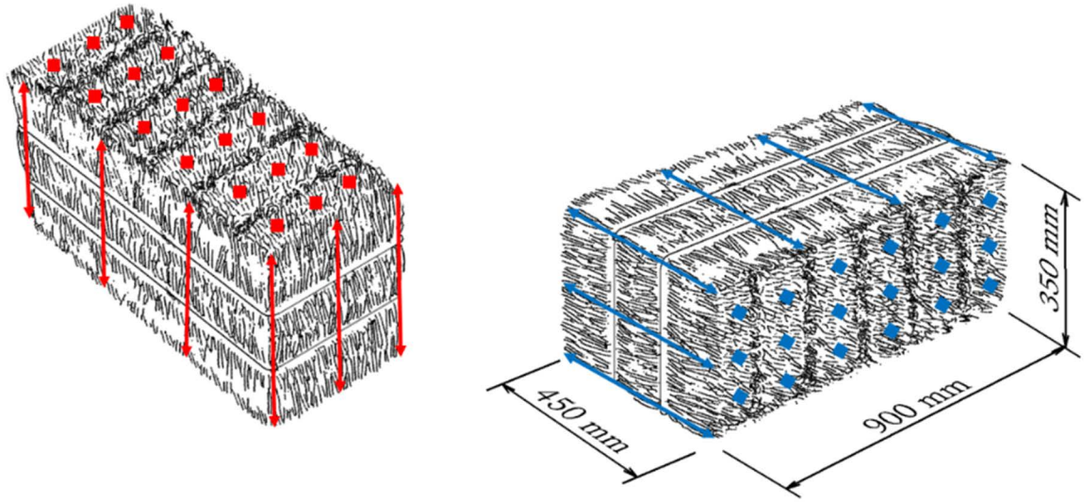

bales. This raises concerns as to the reliability and consistency of the purported properties of straw bale walls.

Unfortunately, there is still a lack of scientific data available in the published literature with regards to the thermal properties of straw bale construction. In addition, for the literature that has been published, most testing programs are not standardized and make it difficult for peers to replicate the testing parameters to confirm the testing data. According to some literature, the thermal performance of straw bale walls can vary depending on the configuration of the wall, including the type of straw, the age of straw, the moisture content, and the orientation of fibers (Stone, 2006). Bale density (Stone 2006) is also purported to affect thermal performance, but there is a lack of supporting data.

Thermal conductivity is typically measured by means of a guarded-hot-plate (ASTM C177-13) or by means of a hot box (ASTM C1363-11). Tables 1 and 2 summarize tests on straw bale reported in the literature.

To date, bales of straw from rice, wheat, and barley with densities ranging between 63 kg/m^3 to 138 kg/m^3 have been tested. Reported values of thermal conductivity range between 0.033 W/mK and 0.1461 W/mK.

Some of this variability can be attributed to the orientation of the straw fibres with respect to the heat flow. McCabe (1993) and FASBA (2009) showed that individual straw bales with fibers oriented perpendicularly (i.e. bales on-edge) to the heat flow are between 20% to 35% less thermally conductive than bales with fibers oriented parallel (i.e. bales flat). This can be attributed to the more direct conductive path through the fibers in bales laid flat as opposed to the discontinuity between fibers in bales laid on-edge (McCabe, 1993). CEC/ATI (1997) performed tests on 2 plastered straw bale walls and found a much larger difference (55%), however, the wall with bales laid flat was found to have significant voids, inflating its thermal conductivity. However, comparing the perpendicular fiber test of CEC/ATI (1997) with the parallel fiber test of Christian et al. (1998), which was conducted using bales with density and

TABLE 1. Summary of hot-plate testing of straw bale as reported in the literature.

Year	Authors	Straw Type	Moisture Content	Density (kg/m^3)	Fiber Orientation	Bale [+Plaster] Thickness (mm)	λ (W/m K)
1993	McCabe	Wheat	8.4%	133	Perpendicular	419	0.04727
					Parallel	584	0.06053
1995	Watts et al.	—	—	—	—	467 [N/A]	0.093
2003	Ashour	Wheat	—	82–138	—	—	0.033
		Barley		69–98			0.034
2004	Beck et al.	Barley	—	80	Perpendicular	22	0.041
2004	CEBTP	—	0%	80	—	50–100	0.0645
			16%				0.0675
			23%				0.0705
2009	FASBA	Wheat	0%	81–111	Perpendicular	—	0.0440
				105	Parallel	—	0.0670
2011	Vėjelienė et al.	Barley	—	65.2	Parallel	100	0.0645
2012	Shea et al.	Wheat	R.H. 50	63–123	—	300	0.0594–0.0642

TABLE 2. Summary of hot-box testing of straw bale panels as reported in the literature.

Year	Authors	Straw Type	Moisture Content	Density (kg/m^3)	Fiber Orientation	Bale [+Plaster] Thickness (mm)	λ (W/m K)
1997	CEC/ATI	Rice	11%	107	Perpendicular	406 [+ 51]	0.0811
					Parallel	584 [+76]	0.1471
1998	Christian et al.	Wheat	13%	128	Parallel	483 [N/A]	0.0995
2004	CEBTP	—	—	—	—	360 [+40]	0.095
2012	Shea et al.	Wheat	—	115	Random	490 [include]	0.087
2016	Conti et al.	Wheat	12.5%	65.7	Parallel	530	0.062
			11.5%	84.1			0.070

FIGURE 3. Manufactured baling process (left) and manufactured high density bale vs. regular 2-string bale (right) (Source: Olds Agtech Industries, 2008).

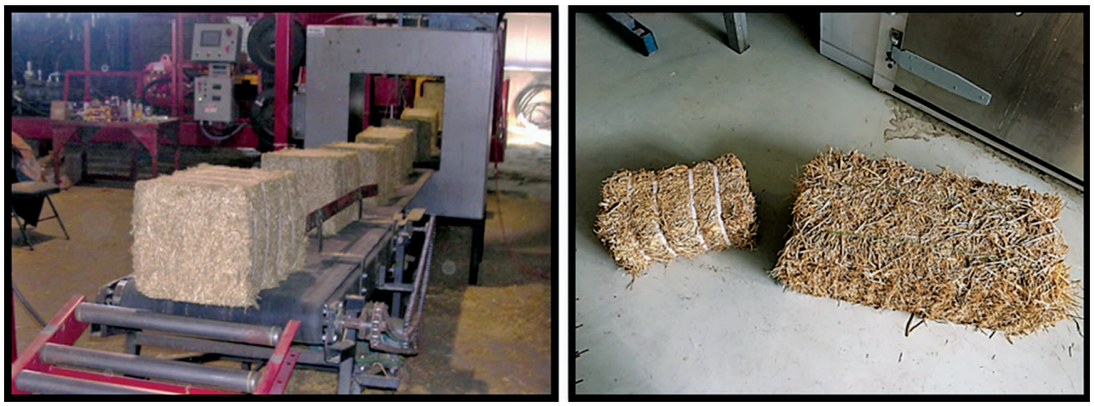

moisture content similar to the CEC/ATI test, there is still close to a 20% decrease in thermal conductivity for plastered straw bales with parallel fibers.

Another important parameter that affects the thermal performance of straw bale panels is the presence of plaster. The results indicate that *unplastered* straw bales are less thermally conductive (i.e make better insulation) than *plastered* straw bales: 45% less for straw fibres oriented *perpendicular* to heat flow, i.e. bales on-edge (on average, as based on McCabe 1993, Beck et al. 2004, FASBA 2009) and 35% less for straw fibres oriented *parallel* to heat flow, i.e. bales flat (on average, as based on McCabe 1993, FASBA 2009, Vejeliene et al. 2011). Moisture has some impact on thermal conductivity, with CEBTP (2004) finding that the thermal conductivity of straw increases 10% as moisture content increased from 0% to 23%. On the other hand, Ashour (2003) found little difference in the thermal conductivity of similar wheat and barley bales.

Straw bales obtained directly from the "field" can have widely varying densities. The international market for forage products has led to the development of "high-density manufactured" bales that can be produced to specified dimensions and densities (Figure 3). Densities of well over 300 kg/m^3 can be achieved. In addition, the straw fibres are much more randomly distributed as compared to field bales. Thus, there is no clear "flat" or "on-edge" orientation with these bales. A long-held concern has been whether straw bale density affects the thermal performance. Shea, Wall & Walker (2012) and FASBA (2009) conducted tests on bales with densities ranging between 63 kg/m^3 and 123 kg/m^3 and found differences in thermal conductivity of only 8%. However, these densities are less than half that of high-density manufactured bales.

The high-density manufactured bales could offer some important advantages for straw-bale builders, including more quality control of dimensions, density, and moisture content. However, the thermal performance of walls constructed using bales of this type cannot be extrapolated from previous tests. If builders want to use these high-density manufactured bales, thermal testing is needed.

OBJECTIVES

There has been no thermal testing reported in the literature of straw bale panels constructed with high-density manufactured bales. It is important to determine if the very high density of

these bales and random fibre orientation affects the thermal conductivity. The objectives of the current study are:

1. Determine, experimentally, the thermal conductivity of panels constructed with high-density (greater than 300 kg/m^3) manufactured straw bales. The testing of full-scale panels will be conducted by means of a "hot box" apparatus, following ASTM C1363-11 as a guideline.
2. Determine if there is a significant difference in the thermal conductivity of straw-bale panels using high-density bales and the thermal conductivity of straw-bale panels using "normal density" (approximately 100 kg/m^3) bales.
3. Determine if there is a significant difference in the thermal conductivity of straw-bale panels using high-density bales and the thermal conductivity of straw-bale panels reported in the literature.

Experimental Program

The experimental program is intended to evaluate the effect of bale density on the thermal performance of plastered straw bale panels by means of a hot box, following ASTM C1363-11 as a guideline. The experimental program started by characterizing the heat losses of the system using two (2) characterization panels at various temperature differentials. Next, three (3) identical, regular density, plastered field straw bale panels were evaluated to correlate the experimental results with the literature. Another medium density plastered field straw bale panel was evaluated. Then, an additional three (3) plastered manufactured straw bale panels with increasing densities were tested.

Specimens and Parameters

Two (2) characterization and seven (7) plastered straw bale panels were fabricated between January and May 2014 by Seitz & MacDougall (2015). Table 3 and Table 4 summarizes the specifications of the characterization panels and thermal straw bale panels, respectively. The panels' dimensions are 1,372 × 1,181 × 410mm (C1, S1, S2, S3, & S4) and 1,372 × 1,067 × 359mm (C2, S5, S6, & S7). The difference in panel thickness was a result of the dimensions available by the bale manufacturer at the time of construction. Note that typical wall panels as installed in a building will be about 2,400 × 2,400 mm. The test specimen panels have been scaled down to permit testing in an available environmental chamber.

The characterization panels were fabricated with a combination of 38.1mm and 25.4mm expanded polystyrene (EPS) board insulation corresponding to the 410mm and 359mm straw bale panel thicknesses (Figure 4). The thermal conductivity of the EPS boards was retrieved from the product's manufacturing label.

Panels S1, S2 and S3 are composed of regular density (90 kg/m^3), 457 × 356 × 838mm 2-string barley bales laid on-edge with nominally a 25.4mm thick layer of lime-cement plaster

TABLE 3. Specifications of the characterization panels.

Panel ID	Infill	Height (mm)	Width (mm)	Depth (mm)	λ (W/m K)
C1	EPS	1,372	1,181	410	0.0386
C2			1,066	359	

TABLE 4. Specifications of plastered straw bale panels.

Panel ID	Infill	Moisture Content	Density (kg/m^3)	Fiber Orientation	Height (mm)	Width (mm)	Bale [+Plaster] Thickness (mm)
S1	Barley	7–8%	89.5	Perpendicular	1,372	1,181	356 [+54]
S2			90.1				
S3			89.6				
S4	Spelt		131				
S5	Wheat		291	Random		1,067	305 [+54]
S6			333				
S7			372				

on both sides. Each panel is composed of three (3) rows of one full bale and one half bale, alternating the location of the split.

Panel S4 is composed of medium density (131 kg/m^3), 457 × 356 × 838mm 2-string spelt bales laid on-edge with nominally a 25.4mm thick layer of lime-cement plaster on both

FIGURE 4. Tests specimens: characterization panels C1 (left) and plastered manufactured straw bale panel S5 (right).

sides. Each panel is composed of three (3) rows of one full bale and one half bale, alternating the location of the split.

Panel S5 (Figure 4), S6 and S7 are composed of high density (291–372 kg/m^3), 305 × 305 × 533mm compressed wheat bales laid flat with nominally a 25.4mm thick layer of lime-cement plaster on both sides. Each panel is composed of four (4) rows of two full bales. These bales are tightly compressed that there is no distinctive orientation of the fibers.

Lime-cement plaster was used throughout because it is the most common type of render implemented in straw bale construction.

METHODOLOGY

The hot box utilized for these tests was the hot box (Figure 5 & Figure 6) presented in Seitz & MacDougall (2015). The construction followed as a guideline ASTM C1363-11, a test standard for the *thermal performance of building materials and envelope assemblies by means of a hot box apparatus*. The standard describes a metering box with 5-sides of known insulation, and the test specimen installed on the 6th side. The energy required to keep the inside of the box at a steady temperature can be used to calculate the thermal resistance of the specimen through the net balance of the heat flow at steady-state, Equation (1):

$$Q_h + Q_f - Q_{mw} - Q_{fl} - Q_{ua} = Q = A \cdot \Delta t / R \tag{1}$$

Where,

Q_h = net heat added by heaters, W
Q_f = net heat added by fans, W
Q_{mw} = metering box wall loss, W
Q_{fl} = flanking loss, W
Q_{ua} = unallocated losses, W
Q = heat flow through the specimen, W
A = metered area of heat flow, m^2
Δt = surface temperature difference across the specimen, K
R = thermal resistance of the specimen, m^2·K/W

In the current testing, the net heat contributed by the heater (Q_h) was measured using a Microswitch CSDC1DA current sensor and recording the time a 150W light bulb was on inside the metering chamber. Effectively, the sensor counts the positive pulses (light bulb on) sent to the data acquisition system at a rate of 120Hz (0.0083sec).

The metering box wall loss (Q_{mw}) corresponds to the heat loss through the five (5) walls of the metering box. Q_{mw} can be estimated with equations (2) and (3) as described in ASTM C1363-11:

$$Q_{mw} = \frac{l_{\text{eff}} A_{\text{eff}} \left(t_{\text{in}} - t_{\text{out}} \right)}{L} \tag{2}$$

$$A_{\text{eff}} = A_{\text{in}} + 0.54 \cdot L \cdot \Sigma e_i + 0.60 \cdot L^2 \tag{3}$$

FIGURE 5. Schematic of hot box apparatus (Seitz and MacDougall, 2015).

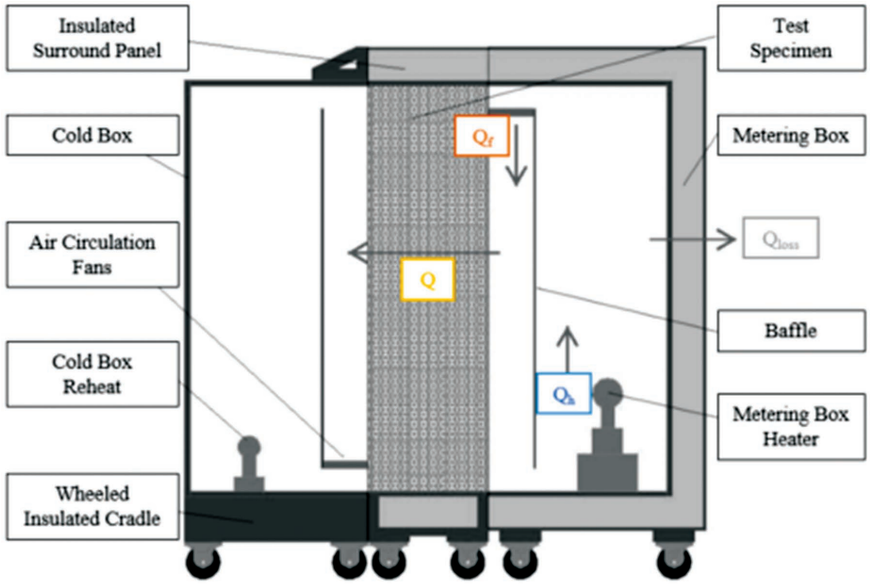

FIGURE 6. Specimen and interior of hot box apparatus (Seitz and MacDougall, 2015).

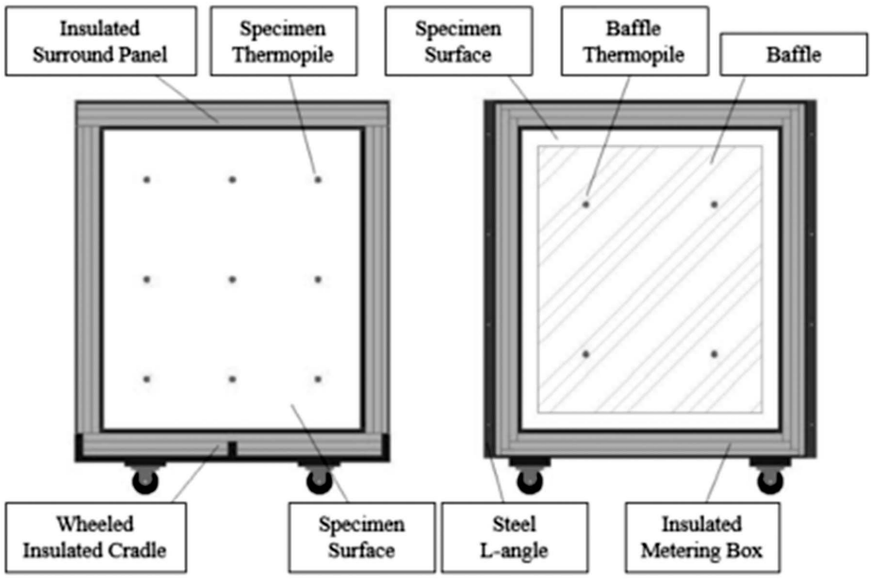

Where,

λ_{eff} = effective thermal conductivity of base insulation and the skin material, W/m K
$\Delta t_{in\text{-}out}$ = inside-to-outside temperature difference across metering chamber walls, K
L = metering chamber wall thickness, m

A_{in} = metering chamber inside surface area, m^2

Σe_i = sum of all metering chamber interior edge lengths formed where two walls meet, m

The flanking loss (Q_{fl}) corresponds to the heat loss at the junction of the specimen and the surround panel. Q_{fl} can be can be estimated with equation (4) as described in ASTM C1363-11:

$$Q_{fl} = \lambda_{eff} \cdot (A/L)_{eff} \cdot \Delta t_{a\text{-}a} \quad (4)$$

Where,

$(A/L)_{eff}$ = effective area/path length of entire frame around its perimeter, m

$\Delta t_{a\text{-}a}$ = air-to-air temperature difference (baffle-to-baffle), K

When performing the characterization tests, the flow through the characterization panel (Q_{cp}) can be determined since the thermal resistance (R) of every wall is known. Using the slope of the linear regression of the characterization data, the total losses (Q_{loss}) of the system can be characterized at designated temperatures. The total losses are initially characterized with equation (5):

$$Q_{loss} = Q_h + Q_f - Q_{cp} \quad (5)$$

The difference between Q_{loss} and the theoretical value, which is the summation of the estimated Q_{fl} and Q_{mw}, will be attributed to unallocated losses (Q_{ua}) that can be associated to estimating error and additional flanking or metering box losses.

Once the characterization is complete, equation (1) can be re-applied but including the total losses of the system and a specimen with an unknown thermal resistance. It is then possible to solve the equation in terms of the heat going through the specimen (Q), which subsequently leads to determining the thermal conductivity with equation (6).

$$\lambda = Q \cdot thick./A \cdot \Delta t \quad (6)$$

Where,

λ = specimen thermal conductivity, W/m K

thick. = specimen thickness, m

"Thermal conductivity" is typically considered a material property, rather than a characteristic of a wall assembly. However, it is being used in this context to compare straw-bale wall panels that are all made with a similar construction technique (i.e. plastered straw bales), and that use straw as the primary insulation material, but that have different panel thicknesses. This makes it a convenient parameter for comparing the thermal performance of the different panels.

Apparatus, Testing Conditions and Instrumentation

As described in Seitz and MacDougall (2015), the hot box apparatus was placed in an environmental chamber (EC) cooled by two controlled chillers. To minimize the impact of air flow created by the chillers, styrofoam baffles were placed in between the chillers and the apparatus in addition to fastening a "cold" box of the same dimensions as the metering chamber to the

specimen's cold face. The cold box and metering chamber were fastened to the specimen by means of four (4) threaded rods on both sides. The face of the surround panel, cold box, and metering chamber included a layer of neoprene sill gasket to help seal the apparatus.

In addition to the specifications prescribed in Seitz and MacDougall (2015), the surround panels were tightly secured to the specimen by two (2) L-angles placed on the outside edges around the entire perimeter of the specimen. A layer of polyethylene vapor barrier was applied on both hot and cold surfaces of the specimen to minimize the potential impact of condensation, which would affect the moisture content inside the specimen.

Seitz and MacDougall (2015) determined that the effective time constant (τ_{eff}), which is the time to reach steady state, is 9 hours. The panels were given sufficient time to eliminate the thermal lag and reach steady-state before recording the data. Three (3) temperature differentials were applied to each specimen with the temperature set at 294.15K (21 °C) for the metering chamber and 279.15K (6 °C), 264.15K (–9 °C), and 249.15K (–24 °C) for the EC. This results in nominal Δt of 15K, 30K and 45K.

The surface temperature is determined by sixty-two (62) Type T 24AWG wired thermopiles with ±0.5 °C instrumentation error. Nine (9) thermopiles were located on the cold surface of the specimen and nine (9) thermopiles were located on the hot surface of the specimen. In addition, four (4) thermopiles were evenly distributed on each cold and hot baffle, three (3) thermopiles were located on the inside and outside of the top, left, right, and bottom wall of the metering chamber and six (6) thermopiles were located on the inside and outside of the back of the metering chamber.

The data acquisition system used for these tests were two (2) MCCDAQ USB-2416 with AI-EXP32 for recording the thermocouples and a custom-fabricated Digital I/O for measuring the heater power input mentioned above. The data was scanned every 2 seconds and the sample average was recorded every 10 seconds resulting in 3,240 data points for a 9-hour test.

The moisture content of the straw infill of panels S3 and S5 were monitored with the Delmhorst FX-2000, which can read between 6–40%, during the subsequent months to determine if the seasonal laboratory environment created any fluctuations in the initial moisture levels.

RESULTS & DISCUSSION

Characterization Panels

Table 5 summarizes the test results for all three characterization panels. The test results from C1-1 were used for tests S1-1, S2-1, S3-1, and S4-1. The test results from C1-2 were used for tests S1-2, S2-2, and S3-2. The test results from C2-1 were used for tests S5-1, S6-1, and S7-1. The total losses for the characterization panels are shown in Figure 7 with the theoretical curve of the metering wall and flanking loss (Q_{mw} + Q_{fl}) estimated with the equations prescribed by ASTM C1363-11.

The net heat added by the fans (Q_f) was initially taken as the manufacturer's specification (17.28W); however, duplicating a test with and without fans showed that the fans were not performing as specified. Disregarding the effect of top-to-bottom surface temperature differential created by eliminating the fans, the heater should input an additional 17.28W when a test is run with no fans. However, when tests S5-1 & S5-NF and S6-1 & S6-NF were run without fans, the additional energy ranged between 3.61W to 7.19W, much lower than the anticipated 17.28W. Therefore, the net heat added by the fans (Q_f) was calculated by making the following

TABLE 5. Summary of data from testing of the characterization panels.

Test ID		C1-1						C1-2						C2-1					
Set Temp.	°C	6		–9		–24		6		–9		–24		6		–9		–24	
			σ		σ		σ		σ		σ		σ		σ		σ		σ
Q_h	W	**15.7**	0.74	**51**	0.94	**85**	1.95	**19.7**	0.69	**53**	0.78	**81.9**	1.16	**21**	0.73	**50**	0.94	**87**	1.24
% of flow		32%		42%		45%		34%		43%		45%		35%		42%		45%	
Q_f	W	**9.17**		**9.17**		**9.17**		**9.3**		**9.3**		**9.3**		**9.10**		**9.10**		**9.10**	
% of flow		18%		8%		5%		16%		7%		5%		15%		8%		5%	
A_{in}	m^2	4.70		4.70		4.70		4.70		4.70		4.70		4.70		4.70		4.70	
L	m	0.133		0.133		0.133		0.133		0.133		0.133		0.133		0.133		0.133	
λ_{eff}	W/mK	0.05		0.05		0.05		0.05		0.05		0.05		0.05		0.05		0.05	
t_{hm}	°C	22.4	3.41	22.4	3.63	21.7	3.91	22.9	3.86	22.6	4.12	22.6	4.56	22.8	3.86	22.3	4.07	22.1	4.32
t_{cm}	°C	10.0	2.53	–5.0	2.69	–19.9	2.88	9.5	3.56	–4.4	3.25	–18.5	3.88	9.3	3.04	–4.2	3.01	–18.9	3.20
$(t_{hm} - t_{cm})$	K	12.4		27.4		41.6		13.4		27.0		41.1		13.5		26.5		40.9	
Σe_i	m	7.518		7.518		7.518		7.518		7.518		7.518		7.518		7.518		7.518	
A_{eff}	m^2	5.25		5.25		5.25		5.25		5.25		5.25		5.25		5.25		5.25	
Q_{mw}	W	**22**		**50**		**75**		**24**		**49**		**74**		**24**		**48**		**74**	
% of flow		45%		41%		40%		42%		39%		41%		41%		40%		38%	
λ_{eff}	W/mK	0.04		0.04		0.04		0.04		0.04		0.04		0.04		0.04		0.04	
$(A/L)_{eff}$	m	5.11		5.11		5.11		5.11		5.11		5.11		4.88		4.88		4.88	

t_{hb}	°C	23.0	1.98	23.4	2.03	23.1	2.12	23.7	2.07	23.9	2.11	24.0	2.17	23.4	2.05	23.2	2.09	23.4	2.10
t_{cb}	°C	11.4	0.58	–5.7	0.62	–21	0.68	9.0	0.43	–5.8	0.52	–20	0.62	10.3	0.39	–4.8	0.50	–20	0.57
$\Delta t_{a\text{-}a}$	K	11.6		29.1		43.8		14.7		29.7		44.2		13.1		28.0		43.3	
Q_{fl}	W	**2.3**		**5.7**		**8.6**		**2.91**		**5.9**		**8.71**		**2.5**		**5.3**		**8.16**	
% of flow		5%		5%		5%		5%		5%		5%		4%		4%		4%	
R	m^2K/W	10.53		10.53		10.53		10.53		10.53		10.53		9.21		9.21		9.21	
A	m^2	1.62		1.62		1.62		1.62		1.62		1.62		1.46		1.46		1.46	
t_{hs}	°C	22.5	2.70	22.8	2.79	22.4	2.80	23.0	2.68	22.9	2.80	23.1	3.12	23.1	2.69	22.7	2.78	22.7	2.88
t_{cs}	°C	11.5	2.90	–5.3	3.15	–20.1	3.26	9.0	3.26	–5.5	3.36	–19.8	3.89	10.4	3.04	–4.6	3.25	–19.6	3.49
Δt	K	11.0		28.1		42.5		14.0		28.3		43.0		12.8		27.3		42.3	
Q_{cp}	W	**1.69**		**4.3**		**6.5**		**2.15**		**4.4**		**6.61**		**2.0**		**4.3**		**6.7**	
% of flow		3%		4%		3%		4%		3%		4%		3%		4%		3%	
Q_{loss}	W	**23.1**		**56**		**87**		**27**		**58**		**85**		**28**		**55**		**89**	
% of flow		47%		46%		47%		46%		47%		46%		47%		46%		47%	
Q_{ua}	W	**–1.5**		**9.10**		**16.7**		**–0.3**		**12.4**		**14.9**		**0.8**		**10.7**		**21**	
% error		–6%		1%		4%		–1%		7%		2%		3%		4%		9%	
Slope (linear regression)		**2.037**						**1.990**						**2.088**					
Slope (theoretical)		**2.003**																	

FIGURE 7. Total loss over temperature differential (Characterization curves).

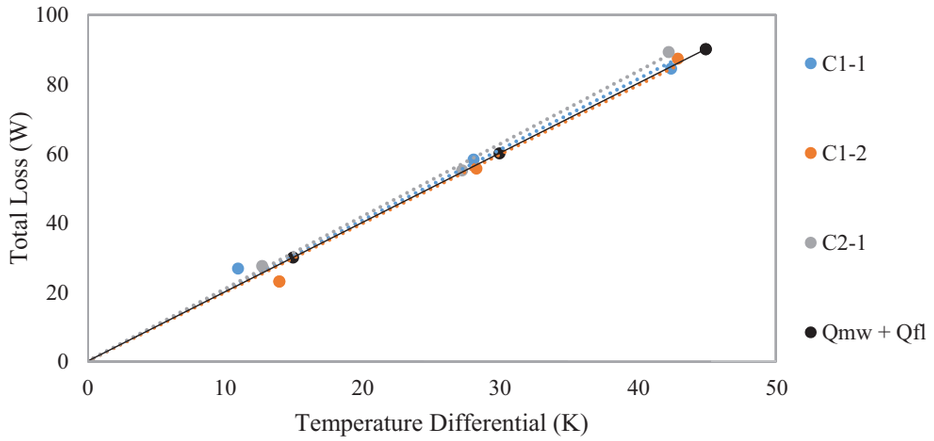

assumptions during the characterization tests. Knowing that the energy inputted by the heater is a linear function with the temperature differential (Δt), Q_f was estimated as the constant energy needed to set the y-intercept of the linear regression of the characterization data to zero losses when $\Delta t = 0$. The reason behind setting the y-intercept to zero is because there should theoretically be no heat transfer when there is no difference in temperature between the walls of the box. These estimated values range from 9.10W to 9.28W, which are more in line with those measured during the tests without fans.

With these assumptions on the energy due to the fans, Figure 7 indicates that the hot box apparatus is behaving as expected with the slopes of the characterization curves having a slope very similar to the theoretical curve with a difference of 1.7%, 0.7%, and 4.2% for test C1-1, C1-2 and C2-1, respectively.

System Sensitivity Analysis

Heat Flow Distribution Comparison for Characterization Panels and Straw Bale Panels

As seen in Table 5, the energy input by the heater (Q_h) for each of the characterization panels increased as the temperature differential decreased. However, it is important to put this energy input in the context of the total energy balance. The proportion of the energy flow through the various components of the hot box and characterization panel (in this case for panel C1-1) is shown in Figure 8. This breakdown shows that although the heat contributed by the fans is constant, relatively speaking, there is a much greater contribution to the energy balance at the low temperature differential (6 °C) than at the higher temperature differentials. This is important because the fan energy, as explained previously, is an estimated value, and any errors in this estimation will therefore affect the precision of the measurement of the thermal conductivity. Figure 8 also shows that the energy flow through the characterization panel is only 3–4% of the total. This means that errors in the measurement of the inputted energy (fans and heater) could have a large impact on the calculation of the thermal conductivity.

Ultimately, the objective of this work is to measure the thermal conductivity of *straw-bale* panels. Tables 6 and 7 summarize the testing of the straw bale panels. Again, the energy input

FIGURE 8. Heat flow distribution for test C1-1.

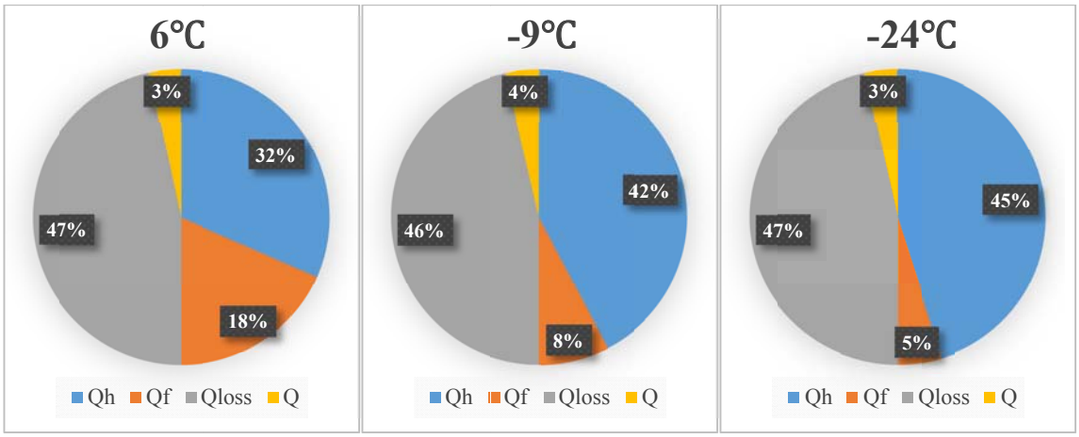

TABLE 6. Summary of data from testing of panels S1, S2 and S3.

Test ID		S1-1						S1-2					
Type		Barley						Barley					
Density	kg/m³	89.5						89.5					
Set Temp.	°C	6		–9		–24		6		–9		–24	
			σ		σ		σ		σ		σ		σ
Q_h	W	**21.5**	**0.76**	**59.5**	**1.22**	**97.1**	**1.38**	**23.2**	**0.73**	**57.6**	**0.67**	**96.6**	**1.43**
% of flow		35%		43%		46%		36%		43%		46%	
Q_f	W	**9.17**		**9.17**		**9.17**		**9.28**		**9.28**		**9.28**	
% of flow		15%		7%		4%		14%		7%		4%	
t_{hs}	°C	22.10	2.79	21.80	2.93	21.59	3.16	22.51	2.73	22.52	2.83	22.03	2.97
t_{cs}	°C	10.82	3.02	–4.64	3.34	–18.8	3.76	9.09	3.21	–4.75	3.41	–18.2	3.57
Δt	K	11.29		26.43		40.41		13.42		27.27		40.27	
Q_{loss}	W	**23.0**		**53.9**		**82.3**		**26.7**		**54.3**		**80.1**	
% of flow		38%		39%		39%		41%		40%		38%	
A	m²	1.62		1.62		1.62		1.62		1.62		1.62	
thick.	m	0.410		0.410		0.410		0.410		0.410		0.410	
Q	W	**7.66**		**14.8**		**23.9**		**5.81**		**13.6**		**25.8**	
% of flow		12%		11%		11%		9%		10%		12%	
λ	W/mK	**0.17**		**0.14**		**0.15**		**0.11**		**0.13**		**0.16**	

(continues)

TABLE 6. Summary of data from testing of panels S1, S2 and S3. *(Cont.)*

Test ID		S2-1						S2-2					
Type		Barley						Barley					
Density	kg/m^3	90.1						90.1					
Set Temp.	°C	6		–9		–24		6		–9		–24	
			σ		σ		σ		σ		σ		σ
Q_h	W	**20.8**	**0.68**	**55.4**	**1.08**	**95.1**	**1.56**	**21.9**	**0.83**	**59.2**	**0.66**	**99.2**	**1.17**
% of flow		35%		43%		46%		35%		43%		46%	
Q_f	W	**9.17**		**9.17**		**9.17**		**9.28**		**9.28**		**9.28**	
% of flow		15%		7%		4%		15%		7%		4%	
t_{hs}	°C	22.47	2.75	22.09	2.92	21.60	3.03	22.65	2.65	22.68	2.78	22.97	3.30
t_{cs}	°C	11.23	3.06	–3.08	3.38	–18.5	3.66	9.69	3.10	–4.52	3.36	–18.8	4.00
Δt	K	11.24		25.17		40.15		12.96		27.20		41.82	
Q_{loss}	W	**22.9**		**51.3**		**81.8**		**25.8**		**54.1**		**83.2**	
% of flow		38%		40%		39%		41%		40%		38%	
A	m^2	1.62		1.62		1.62		1.62		1.62		1.62	
thick.	m	0.410		0.410		0.410		0.410		0.410		0.410	
Q	W	**7.02**		**13.3**		**22.5**		**5.40**		**14.4**		**25.2**	
% of flow		12%		10%		11%		9%		10%		12%	
λ	W/mK	**0.16**		**0.13**		**0.14**		**0.11**		**0.13**		**0.15**	

by the heater (Q_h) for each of the straw bale panels increased, as would be expected, as the temperature differential decreased. Figure 9 shows the proportion of the energy flow through the various components of the hot box for a straw-bale panel test (in this case for panel S1-1). A key observation is that energy flow through the straw-bale panel is much higher than through the equivalent characterization panel, comprising 11–12% of the total.

As noted by Buratti et al. (2016), the thermal resistance of the characterization panel has an impact on the accuracy of the total loss estimation. The characterization panels were constructed to be dimensionally as close as possible to the straw test specimen panels; however, this resulted with the characterization panels being much more thermally resistant than the straw test specimen panels.

Conceptually, the impact of this on the thermal conductivity calculations can be assessed by considering the analogy between the heat flow and water flow. Consider a 4-sided box filled with water, and in **Scenario 1)** the box has three walls that are *highly permeable* and one wall that has *low permeability*. In **Scenario 2)** all four walls of the box are *highly permeable*. The volume of water going through the three highly permeable walls in Scenario 2 will be much lower than the volume of water going through the walls in Scenario 1. Relating this to the thermal tests,

TABLE 6. Summary of data from testing of panels S1, S2 and S3. *(Cont.)*

Test ID		S3-1						S3-2					
Type		Barley						Barley					
Density	kg/m^3	89.6						89.6					
Set Temp.	°C	6		–9		–24		6		–9		–24	
			σ		σ		σ		σ		σ		σ
Q_h	W	**19.7**	**0.83**	**55.5**	**1.43**	**98.4**	**1.00**	**21.1**	**0.98**	**60.2**	**0.90**	**102**	**0.98**
% of flow		34%		43%		46%		35%		43%		46%	
Q_f	W	**9.17**		**9.17**		**9.17**		**9.28**		**9.28**		**9.28**	
% of flow		16%		7%		4%		15%		7%		4%	
t_{hs}	°C	22.09	2.76	21.82	2.83	22.15	3.04	22.57	2.70	22.32	2.88	22.66	3.15
t_{cs}	°C	11.07	3.04	–4.11	3.27	–19.2	3.54	9.44	3.03	–4.96	3.31	–19.0	3.63
Δt	K	11.02		25.93		41.33		13.13		27.28		41.70	
Q_{loss}	W	**22.5**		**52.8**		**84.2**		**26.1**		**54.3**		**83.0**	
% of flow		39%		41%		39%		43%		39%		37%	
A	m^2	1.62		1.62		1.62		1.62		1.62		1.62	
thick.	m	0.410		0.410		0.410		0.410		0.410		0.410	
Q	W	**6.46**		**11.8**		**23.3**		**4.25**		**15.2**		**28.1**	
% of flow		11%		9%		11%		7%		11%		13%	
λ	W/mK	**0.15**		**0.12**		**0.14**		**0.08**		**0.14**		**0.17**	

the characterization curves were determined under Scenario 1, but the straw bale specimens resembled Scenario 2. Based on the heat distribution portrayed in Figure 8 and Figure 9, one can see the difference between the heat distribution of C1-1 and S1-1; subsequently, this will reduce the accuracy of the C1-1 characterization curve when it is used to determine the total losses for S1-1 (and for all the other straw bale panels as well). Therefore, the thermal conductivity values for straw bale panels presented in this paper should not be considered the "true" values, but rather the relative values in comparison to each other.

Error Propagation Analysis for Thermal Conductivity Calculations

Figure 10 displays a sample of the raw data for panel C1-1 at 6 °C and it clearly shows that the apparatus can maintain steady-state conditions, on average, over the 9 hour time constant. Some spikes in the power readings were observed, however, these had limited impact on the average Q_h. However, the fluctuation of the hot and cold specimen surface temperature is quite significant. The standard deviation of the recorded surface temperatures fluctuates between 2.7K and 4K. This will subsequently affect the precision of the characterization curve used to calculate the total losses of the system.

TABLE 7. Summary of data from testing of panels S4, S5, S6, and S7.

Test ID		S4-1						S5-1						S6-1						S7-1					
Type		Spelt						Wheat						Wheat						Wheat					
Density	kg/m^3	131						291						333						372					
Set Temp.	°C	6		–9		–24		6		–9		–24		6		–9		–24		6		–9		–24	
			σ		σ		σ		σ		σ		σ				σ				σ				σ
Q_h	W	**20.5**	**0.68**	**59.2**	**1.40**	**97.0**	**1.26**	**18.6**	**0.35**	**62.1**	**1.01**	**95.4**	**0.89**	**19.3**	**0.73**	**61.0**	**1.07**	**95.1**	**0.91**	**19.9**	**1.08**	**66.0**	**1.21**	**97.9**	**0.77**
% of flow		35%		43%		46%		34%		44%		46%		34%		44%		46%		34%		44%		46%	
Q_f	W	**9.17**		**9.17**		**9.17**		**9.10**		**9.10**		**9.10**		**9.10**		**9.10**		**9.10**		**9.10**		**9.10**		**9.10**	
% of flow		15%		7%		4%		16%		6%		4%		16%		6%		4%		16%		6%		4%	
t_{hs}	°C	22.08	2.81	21.79	2.92	22.24	3.08	22.18	2.76	22.23	2.77	21.46	2.96	22.18	2.76	21.98	2.81	21.53	2.85	21.87	2.79	21.00	3.01	19.77	3.27
t_{cs}	°C	11.20	3.06	–4.43	3.27	–18.8	3.60	12.77	3.21	–3.17	3.43	–17.2	3.73	11.57	2.96	–4.02	3.17	–17.4	3.35	12.39	3.01	–3.32	3.17	–16.8	3.46
Δt	K	10.88		26.22		41.02		9.41		25.40		38.62		10.61		26.00		38.98		9.49		24.32		36.61	
Q_{loss}	W	**22.2**		**53.4**		**83.6**		**19.7**		**53.0**		**80.7**		**22.2**		**54.3**		**81.4**		**19.8**		**50.8**		**76.5**	
% of flow		37%		39%		39%		35%		37%		39%		39%		39%		39%		34%		34%		36%	
A	m^2	1.62		1.62		1.62		1.46		1.46		1.46		1.46		1.46		1.46		1.46		1.46		1.46	
thick.	m	0.410		0.410		0.410		0.359		0.359		0.359		0.359		0.359		0.359		0.359		0.359		0.359	
Q	W	**7.46**		**14.9**		**22.6**		**8.07**		**18.2**		**23.8**		**6.25**		**15.8**		**22.8**		**9.22**		**24.3**		**30.5**	
% of flow		13%		11%		11%		15%		13%		11%		11%		11%		11%		16%		16%		14%	
λ	W/mK	**0.17**		**0.14**		**0.14**		**0.21**		**0.18**		**0.15**		**0.14**		**0.15**		**0.14**		**0.24**		**0.25**		**0.20**	

FIGURE 9. Heat flow distribution for test S1-1.

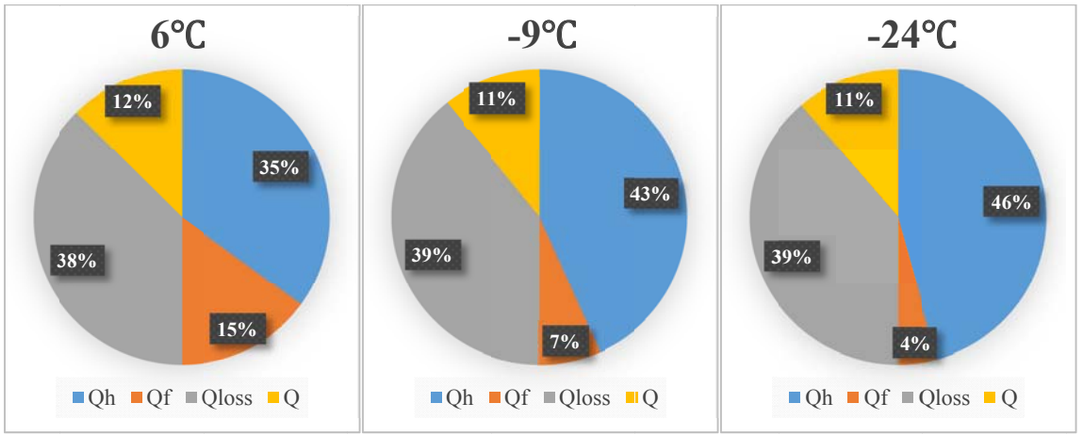

Figure 11 demonstrates the sensitivity of the calculated thermal conductivity for straw bale panel S1-1 to changes in the surface-to-surface temperature differential ($\Delta t_{s\text{-}s}$) of up to ± one standard deviation. The standard deviation of $\Delta t_{s\text{-}s}$ is smaller for lower temperature differentials; however, its impact on the calculated thermal conductivity is much larger because the total input energy is relatively smaller than at higher temperature differentials. The maximum difference from the thermal conductivity value calculated based on the average $\Delta t_{s\text{-}s}$ is ±159% for test S1-2 at 6 °C. The average difference was 68% for all panels at every temperature differential.

The variability in the measured energy input values was relatively small, with typical coefficients of variation between 1% to 4%. Figure 12 shows the sensitivity of the calculated thermal conductivity for straw bale panel S1-1 to ranges in heat flow value of ± one standard deviation. Like the $\Delta t_{s\text{-}s}$ sensitivity, the standard deviation of Q_h is smaller at lower temperature differential; however, its effect on the final thermal conductivity of the panel is much larger. Again, the deviation is larger at the lower temperature differential because the total amount of energy input into the system is relatively small in comparison to the energy at a higher temperature

FIGURE 10. Raw data sample of panel C1-1 at 6 °C.

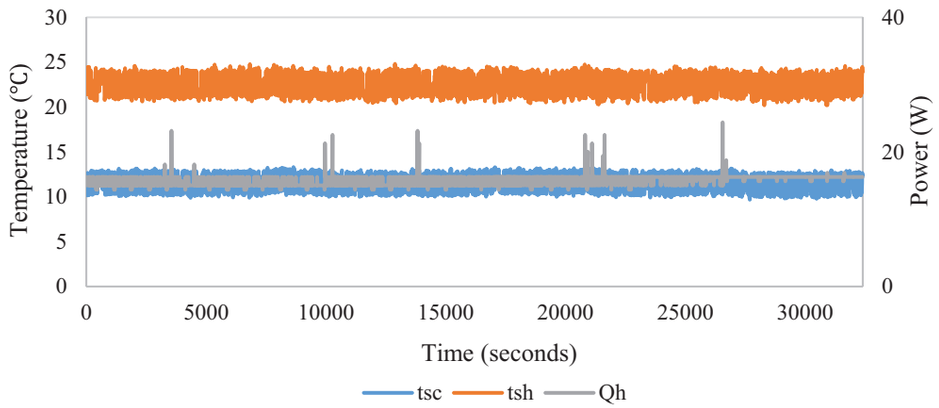

FIGURE 11. Sensitivity of thermal conductivity with respect to surface-to-surface temperature differential for test S1-1.

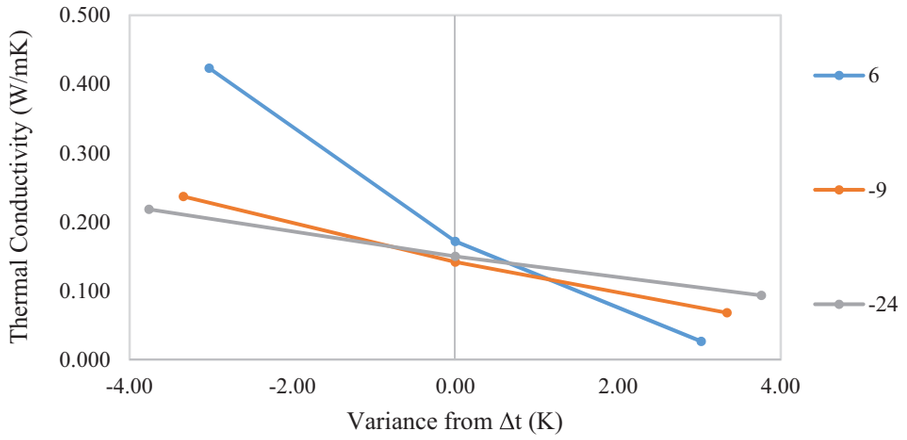

differential. The maximum difference in the thermal conductivity from that calculated using the average Q_h was ±14% for test S7-1 at 6 °C. The average difference for all panels at every temperature differential was 8%.

This analysis indicates that the thermal conductivity calculations are approximately twice as sensitive to $\Delta t_{s\text{-}s}$ variations as to energy measurement variations. This is the case because $\Delta t_{s\text{-}s}$ is multiplied by the slope of the characterization curve, where the theoretical slope is equal to 2.003 W/Δt, as opposed to Q_h which is directly inputted into the energy balance equation. Reducing this slope, which is done by reducing the total losses, would reduce the sensitivity.

Plastered Straw Bale Panels

As the previous analysis indicates, the apparatus is highly sensitive and less reliable at the lower temperature differential. Therefore, when considering the straw bale panels, the results obtained at the 6 °C setting were neglected.

FIGURE 12. Sensitivity of thermal conductivity with respect to heater energy input for test S1-1.

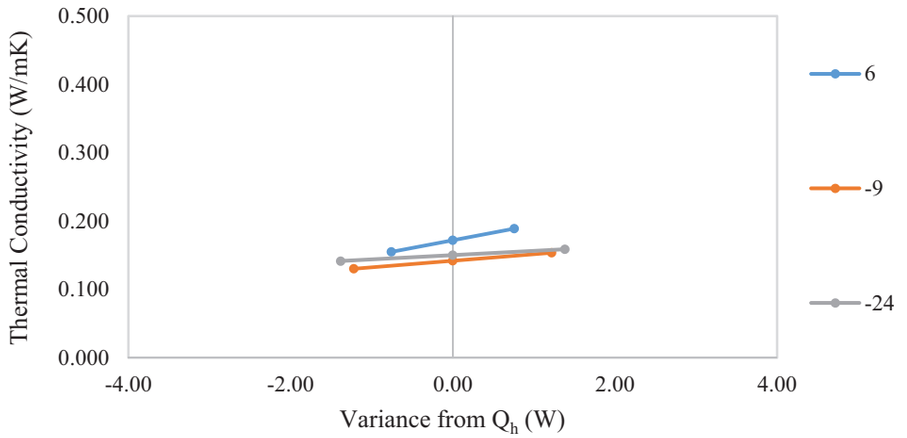

FIGURE 13. Average thermal conductivity of each panel for –9 °C and –24 °C versus the bale density.

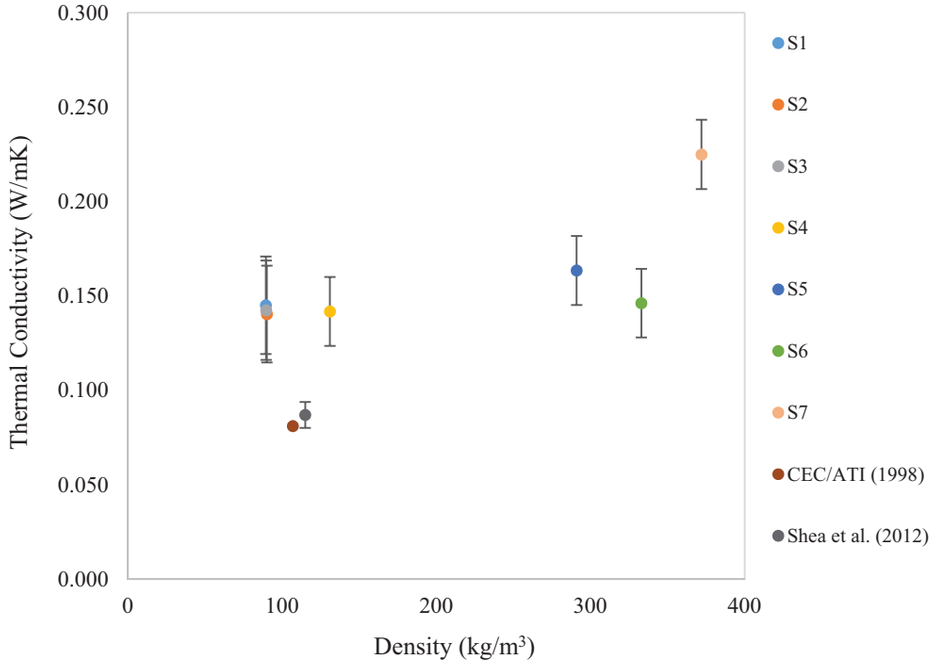

Table 6 summarizes the results obtained for the plastered straw bale panels S1 to S3 and Table 7 for panels S4 to S7. In Figure 13, thermal conductivity values are plotted with respect to bale density. The error bars associated with the data in Figure 13 indicates the error propagated through the thermal conductivity calculations due to the scatter in temperature and heat input measurements.

Panels S1, S2 and S3 were manufactured with 90 kg/m^3, 2-string barley bales laid on-edge. Their average thermal conductivity is 0.143 ± 0.045 W/mK. CEC/ATI (1998), CEBTP (2004) and Shea et al. (2012) reported thermal conductivity values for plastered straw bale panels with fibers oriented perpendicular or randomly with respect to heat flow. The thermal conductivity results obtained from CEC/ATI (1998) and Shea et al. (2012) have been plotted with the thermal conductivity results obtained in this experimental program against the bale density in Figure 13. CEBTP (2004) was left out because the bale density and fiber orientation were not recorded; however, the reported thermal conductivity value was 0.095 W/mK.

The average experimental thermal conductivity values for S1, S2, and S3 are 76% and 64% larger than CEC/ATI and Shea et al.'s reported values, respectively. The larger thermal conductivity measured in this experimental program can be attributed to voids discovered inside the panels. Following the thermal tests, and upon dismantling the panels, voids as large as 300mm were uncovered along the perimeter of the plaster of the regular density panels and at the joints between the bales of the high density panels (Figure 14). These voids are believed to have been a result of the "scaled-down" panels that were used in the testing, which made it more difficult to accommodate the typical bale sizes. These voids are large enough that natural convection could occur, permitting additional heat flow and reducing the panel's effective

FIGURE 14. Side view of panels after testing and with outer timber box removed.

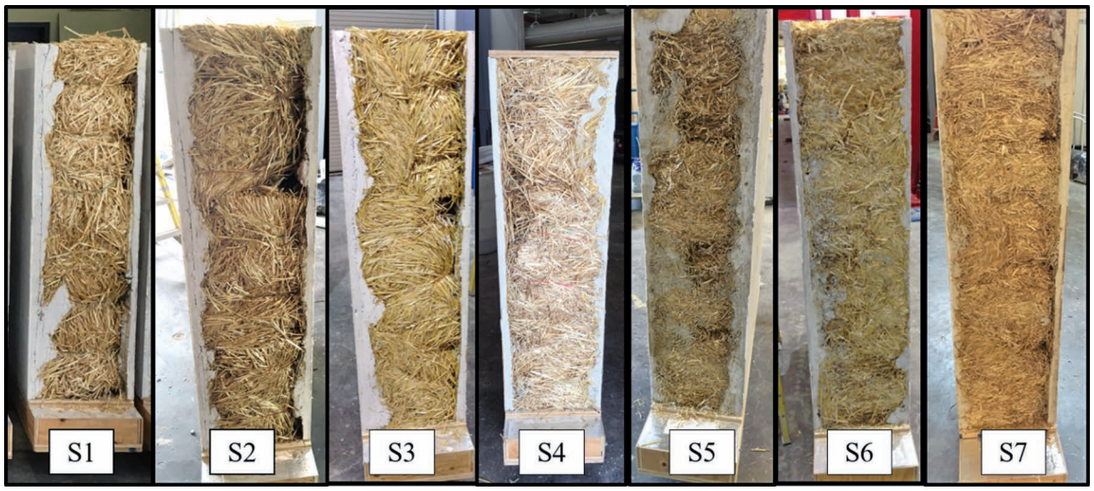

thermal conductivity (Straube, 2011). It would be expected that in a normal sized wall panel, builders would ensure these voids have been filled, and the thermal conductivity would thereby approach values reported by CEC/ATI and Shea et al.

Nevertheless, the results in Figure 13 can be used to compare the thermal conductivity of straw bale panels with 'normal density' bales (S1, S2, S3, S4) and high-density manufactured bales (S5, S6, S7). Within the experimental error, and up to a density of 333 kg/m^3 (S6), there does not appear to be a discernable difference in thermal conductivity as bale density increases. There is also no discernable difference in the thermal conductivity of panels made with conventional bales orientated flat, and the panels made with the high-density manufactured bales.

FIGURE 15. Example of voids in tested straw-bale panels: 40mm × 100mm void through S5 (left) and 60mm × 35mm void through S7 (right).

An exception is specimen S7 made with manufactured bales of density 372 kg/m^3, and which has a significantly higher thermal conductivity than the other panels. It is possible that S7 is an outlier; however, it may also indicate a transition point where the straw bale density is affecting thermal conductivity.

SUMMARY & CONCLUSIONS

This paper described the hot-box testing of seven straw bale wall panels to obtain their thermal conductivity values. Four panels were made with traditional, 2-string bales of 'normal density' (89.5 kg/m^3–131 kg/m^3) and with the bales on-edge (fibres perpendicular to the heat flow). Three panels were made with manufactured high-density bales (291 kg/m^3–372 kg/m^3). The fibres of the manufactured bales were randomly oriented. There were three objectives for the testing, including 1) determining the thermal conductivity of panels with high density bales, 2) determining if there is a significant difference in the thermal conductivity of panels with high density and normal density bales, and 3) determining if there is a difference in the thermal conductivity for panels with high density bales and values reported in the literature. Only Objective 2 was met. The key conclusion of this paper is that within the experimental error, there is no difference in the thermal conductivity value for panels using normal density bales and manufactured high density bales up to a density of 333 kg/m^3. However, because of lack of precision of the hot-box, no conclusions can be made on the true thermal conductivity of the high density bale panels. In addition, the panels tested were found to have significant voids between bales, and this is believed to have contributed to higher measured thermal conductivity values compared to those reported in the literature for normal density bale panels. Thermal properties may be affected for bales with higher densities than 333 kg/m^3, therefore further testing is suggested.

REFERENCES

Architectural Testing Inc. (1997). *Thermal Performance (ATI-20227)*. Fresno, California, USA: California Energy Commision.

Ashour, T. (2003). *The use of renewable agricultural by-products as building materials*. Egypt: Benha Iniversity.

ASTM International. (2015). *ASTM C168-15a Standard Terminology Relating to Thermal Insulation*. West Conshohocken, PA.

Beck, A., Heinemann, U., Reidinger, M., & Fricke, J. (2004). Thermal Transport in Straw Insulation. *Journal of Thermal Envelope and Building Science, 27*(3), 227–234.

Blanchard, S., & Reppe, P. (1998). *Life cycle analysis of a residential home in Michigan*. University of Michigan, School of Natural Resources and Environment.

Buratti, C., Belloni, E., Lunghi, L., & Barbanera, M. (2016). Thermal Conductivity Measurements By Means of a New 'Small Hot-Box' Apparatus: Manufacturing, Calibration and Preliminary Experimental Tests on Different Material. *Int J Thermophys*, 37–47.

Carter, G., Jain, P., & Hou, J. (1996). *Report on the Physical Performance of the Real Goods Solar Living Centre Retail Showroom*. University of California at Berkeley.

Christian, J., & Eisenberg, D. (1998). *(Unkown)*. Oak Ridge National Laboratory.

Conti, L., Barbari, M., & Monti, M. (2016). Steady-State Thermal Properties of Rectangular Straw-Bales (RSB) for Building. *Buildings, 6*(44).

Fachverband Strohballenbau (FASBA). (2009). *Thermal performance*. Germany: Strawbale building research development.

Grelat, A. (2003). *Utilisation de la paille en parois de maisons individuelles a ossature bois*. Centre d'expertise du batiment et des travaux public.

ICFHome. (2017, Januray 11). *Straw-Bale Home Construction*. Retrieved from Ontario's Custom Home Builder: http://buildersontario.com/straw-bale-home-construction
King, B. (2006). *Design of straw bale buildings*. San Rafael, California, USA: Green Building Press.
Magwood, C. (2014). *Making better buildings: a comparative guide to sustainable construction for homeowners and contractors*. Canada: New Society Publishers.
McCabe, J. (1993). *The thermal resistivty of straw bales for construction*. University of Arizona.
Morrison, F. (2014). *Obtaining Uncertainty Measures on Slope and Intercept of a Least Squares Fit with Excel's LINEST*. Houghton, MI: Michigan Technological University.
Olds Agtech Industries. (2008, 08 27). *Facebook*. Retrieved 01 25, 2017, from Olds Agtech Industries: https://www.facebook.com/Olds-Agtech-Industries-205085182894121/
Ramesh, T., Prakash, R., & Shukla, K. (2010). Life cycle energy analysis of buildings: An overview. *Energy and Buildings, 42*, 1592–1600.
Sartori, I., & Hestnes, A. (2007). Energy use in the life cycle of conventional and low-energy buildings: A review Article. *Energy and Buildings, 39*, 249–257.
Seitz, S., & MacDougall, C. (2015). Design of an Affordable Hot Box Testing Apparatus. *NOCMAT*. Winnipeg.
Shea, A., Wall, K., & Walker, P. (2012). Evaluation of the thermal performance of an innovative prefabricated natural plant fibre building system. *Building Serv. Eng. Res. Technol., 0*(0), 1–12.
Stone, N. (2006). Thermal Performance of Plastered Straw Bale Walls. In B. King, *Design of Straw Bale Building: The state of the art* (pp. 185–194). San Rafael, California, USA: Green Building Press.
Straube, J. (2011). Thermal Control in Buildings. *Building Science Digest* (011).
United Nation Envionmental Programme. (2009). *Buildings and Climate Change*. Paris, France: UNEP DTIE.
Vėjelienė, J., Gailius, A., Vėjelis, S., Vaitkus, S., & Balčiūnas, G. (2011). Evaluation of Structure Influence on Thermal Conductivity of Thermal Insulating Materials from Renewable Resources. *Materials Science, 17*(2), 208–212.
Watts, K., Wilkie, K., Thompson, K., & Corson, J. (1995). Thermal and mechnical properties of straw bales as they relate to a straw house. *Agricultural Institute of Canada*, (p. 18). Ottawa.

APPENDIX A

List of symbols

A = metered area of heat flow, m^2

A_{in} = metering chamber inside surface area, m^2

$(A/L)_{eff}$ = effective area/path length of entire frame around its perimeter, m

L = metering chamber wall thickness, m

n = sample size

Q = heat flow through the specimen, W

Q_{cp} = heat flow through the characterization panel, W

Q_f = net heat added by the fans, W

Q_{fl} = flanking loss, W

Q_h = net heat added by the heaters, W

Q_{loss} = total loss of system, W

Q_{mw} = metering box wall loss, W

Q_{ua} = unallocated losses, W

R = thermal resistance of the specimen, $m^2 \cdot K/W$

SE = standard error of sample

slope = slope of linear regression of the characterization data, W/K

thick. = specimen thickness, m

t_{hs} = average hot surface temperature of specimen, °C

t_{cs} = average cold surface temperature of specimen, °C

t_{hm} = average metering chamber inside wall surface temperature, °C

t_{cm} = average metering chamber outside wall surface temperature, °C

t_{hb} = average metering chamber baffle surface temperature, °C

t_{cb} = average cold chamber baffle surface temperature, °C

Δt = surface temperature difference across the specimen, K

$\Delta t_{\text{in-out}}$ = inside-to-outside temperature difference across metering chamber walls, K

$\Delta t_{a\text{-}a}$ = air-to-air temperature difference (baffle-to-baffle), K

λ = specimen thermal conductivity, W/m K

λ_{eff} = effective thermal conductivity of base insulation and the skin material, W/m K

Σe_i = sum of all metering chamber interior edge lengths formed where two walls meet, m

σ = standard deviation of the sample